



## Adsorption of Zinc in Aqueous Solution onto Natural Maghnite Modified by 3-Aminopropyltriethoxysilane

Mohamed Amine Zenasni<sup>1,2,3,\*</sup>, Bahia Meroufel<sup>1,3</sup>, Said Benfarhi<sup>2</sup>  
André Merlin<sup>3</sup>, Stéphane Molina<sup>3</sup>, Béatrice George<sup>3</sup>

<sup>1</sup> Institute of Sciences and Technology, Department of Sciences, Bechar University, Bechar, Algeria;

<sup>2</sup> Institute of Sciences, Department of Chemistry, Batna University, Batna, Algeria

<sup>3</sup> Laboratory of Studies and Research on Material Wood (LERMAB), University of Lorraine, Nancy, France.

Received 07 July 2014; Revised 10 October 2014; Accepted 12 October 2014.

\* Corresponding Author. Email: [am.zenasni@gmail.com](mailto:am.zenasni@gmail.com)

### Abstract

Zinc (II) was immobilised directly onto clay, maghnite (M13), and after their amine functionalisation with (3-aminopropyl)triethoxysilane (APTES). The APTES-functionalised maghnite (MS) showed higher zinc loading than only maghnite, indicating that the clay functionalisation enhanced the Zn(II) removal. The hydrophilic properties of the clay surface have been modified, but not turned into hydrophobic ones. The graft has indeed a polar amine group and the chain length is too short to present an important hydrophobic character. X-ray diffraction indicated that their original structure had been preserved. This new hybrid organic-inorganic material may be a good alternative for separation and pre-concentration of heavy metal ions. Both adsorbents were characterised by FTIR, XRD, TG and SEM. Both adsorbents showed maximum adsorption of the metal ions at pH 6.1 for Mag and pH 9 for MS. The adsorption processes followed pseudo-second-order kinetics. The Langmuir model best fits the adsorption data.

*Keywords:* Maghnite, APTES, Zinc, Hydrophil, Intercalation, Adsorption.

### 1. Introduction

Over the years, the percolation of heavy metals into the water bodies and ecosystem remain as one of the most elusive and pervasive environmental threat to the global occupants. Heavy metal ions are classified as priority pollutants based on their toxicity and mobility in natural water streams. Nevertheless, the heavy metal ions are stable and persistent to environment changes since they cannot either be degraded or destroyed [1]. The increment of industrialization has aggravated the situation due to the mass loading of highly concentrated metal ions containment effluent into the waterways.

To date, various treatment approaches have been applied by scientific community in order to decontaminate the water free from any heavy metal ions. These methods including adsorption, complexation, chemical oxidation or reduction, chemical precipitation, reverse osmosis, ion exchange, solvent extraction, membrane filtration, coagulation, phytoextraction and evaporation [2]. Adsorption is one of the most cost-effective methods due to its ease to operate, high efficiency and low maintenance cost whereas other treatment alternatives may have some disadvantages such as high consumption of reagent and energy, incomplete metal removal, low selectivity, high operational cost and problem in disposing the secondary waste generated during the treatment process [2]. Activated carbon has been the most respective and widely used adsorbent but it is relatively expensive in price. Therefore, this scenario has prompted the exploration of low cost adsorbent to be used as replacement for activated carbon.

The feasibility and reliability of lignocellulosic biomass, natural clay minerals and biological-based materials used as low cost adsorbent has been evaluated by many researchers. These materials including sugarcane bagasse, risk husk, tea leaves, bamboo dust, maize cob, tree sawdust [3], zeolite [4,5], bentonite [6,7],

montmorillonite [8], kaolin [9], *Cephalosporium aphidicola* [10], *Pinus sylvestris* [11], *Saccharomyces cerevisiae* [12], and so forth.

Availability of clay in nature and its high potential toward the adsorption of organic and inorganic compounds has attracted the attention of many researchers to use it for the removal of pollutants [13, 14]. The removal of heavy metals by natural adsorbent has become one of the most suitable solutions for environmental remediation. Natural clay is also available in Algeria and its potential use in the present context is very limited [15].

In this work, we collected clay from the Maghnia formation Algeria (named Maghnite), and used as natural adsorbent for the removal Zn (II) in aqueous systems. The modification process for this clay is based on the strategy commonly used for maghnite functionalization. It consists of a direct condensation reaction between 3-aminopropyltriethoxysilane (APTES) and the hydroxyl groups of the clay minerals. The material was characterized by X-ray diffraction (XRD) and scanning electron microscopy (SEM).

The present work aims also critically review information concerning the factors that impact the adsorption and ion exchange, the system kinetics and equilibrium with respect to various models that have been applied in the literature. Much of the information summarized in this work has been tabulated; this way it is easy to compare the experimental conditions and results of various works. Since both ion exchange and adsorption are usually involved in the uptake of heavy metals by natural and modified clay, in the context of this work hereafter the term adsorption also includes the ion exchange that takes places. In practical applications, adsorption and ion exchange can be grouped together as sorption for a unified consideration.

## 2. Materials and methods

### 2.1. Materials

#### 2.1.1. Clay Minerals

The maghnite used in this work came from a quarry located in Maghnia (North West of Algeria) and was supplied by company "ENOF" (an Algerian manufacture specialized in the production of nonferrous products and useful substances). The different chemical elements of the native maghnite were transformed into oxides and analysed by X-ray fluorescence (experiment carried out at ENOF). Results are given in Table 1. These results confirm that the maghnite used consists essentially of montmorillonite, since the ratio  $\text{SiO}_2/\text{Al}_2\text{O}_3$  is equal to 3.77 and thus belongs to the family of the phyllosilicates. This maghnite form is stable suspensions in water and had flat platelets or needlelike structures. Granulometry of the crude maghnite have been prepared in the Civil Engineering Department of Tlemcen University (EDTU) in Algeria using a sedimentation technique with a 0.1% solution of sodium hexametaphosphate; 95% of the particles were found to have a diameter of less than 80  $\mu\text{m}$ . The cation exchange capacity was measured to be 101.25 meq/100g of clay, and the surface area was 27  $\text{m}^2/\text{g}$ , with an average pore size of 7 nm. [19]

**Table 1.** Chemical composition of the maghnite.

Species	$\text{SiO}_2$	$\text{Al}_2\text{O}_3$	$\text{Fe}_2\text{O}_3$	CaO	MgO	$\text{Na}_2\text{O}$	$\text{K}_2\text{O}$	$\text{TiO}_2$	L.O.I*
% (w/w)	65.20	17.25	2.10	1.20	3.10	2.15	0.60	0.20	8.20

\* L.O.I : Loss on ignition

#### 2.1.2. Reagents

The reagents used in this study were all extra pure analytical grades: The (3-aminopropyl) triethoxysilane (APTES) was purchased from Sigma-Aldrich, China.  $\text{ZnSO}_4 \cdot 7\text{H}_2\text{O}$ , was purchased from Fisher Scientific (Pittsburgh, PA). Toluene and ethanol were of analytical grade. Distilled water was used in all experiments. The pH of solution was adjusted by using 0.1 M NaOH and/or 0.1 M HCl.

### 2.2. Methods

#### 2.2.1. Functionalisation of the Clay with (3-Aminopropyl)triethoxysilane

20.0 g maghnite (dried at 105 °C) was dispersed into 300 mL toluene by ultrasound for 15 min. Then, 20.0 mL APTES was added dropwise during vigorous stirring. The dispersion was refluxed at 100°C for 24h. The modified maghnite was centrifuged and washed with toluene, followed by volume mixture between ethanol and distilled water (75/25 v%),

respectively. The product was dried at 105 °C and sieved. The sketch in Fig. 1 shows the grafting process and the structure of Products.

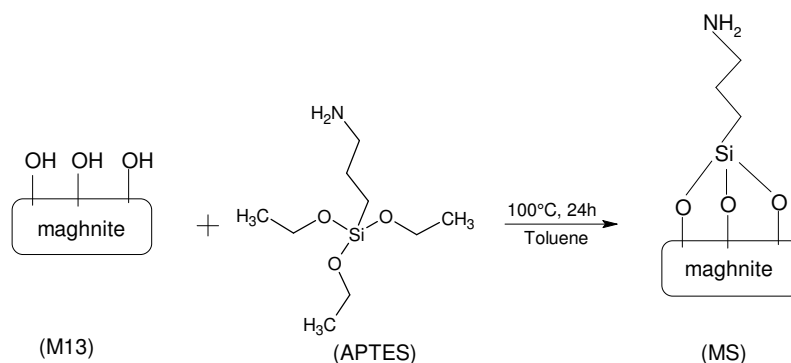


**Figure 1.** Schematic diagram of maghnite modification

### 2.2.2. Adsorption Experiments

The adsorption of metal ion ( $Zn^{2+}$ ) by maghnite (M13) and modified maghnite (MS) was studied. A 0.2 g maghnite (M13) was placed in 20 mL solution of 100 mg/L of  $Zn^{2+}$  at pH6.1 and 0.2 g modified maghnite (MS) was placed in 20 ml solution of 200 mg/L of  $Zn^{2+}$  at pH9. The samples were equilibrated in shaker bath, operating at 25 °C and 100 rpm. After a period of time, the supernatants were collected and quantified for the amount of metal by SAA. The effects of the pH, the contact time, and the initial metal ion concentration on the adsorption capacity of the M13 and MS were examined. The maximum adsorption capacity was calculated from Langmuir and Freundlich isotherms plot. The amount of Zn(II) adsorbed per unit mass of M13 and MS were calculated by using the mass balance equation given in Eq. (1) [16].

$$q_e = (C_0 - C_e)V/m \quad (1)$$

where  $q_e$  is the maximum adsorption capacity in mg/g,  $C_0$  is the initial concentration and  $C_e$  is the concentration at equilibrium of Zn(II) solution in mg/L,  $V$  is the volume of the Zn(II) solution in mL and  $m$  is the mass of the materials in grams.

Adsorption percentage (%) was derived from the difference of the initial concentration ( $C_0$ , mol/L) and the final one ( $C_e$ , mol/L) (eq (2)):

$$Sorption \% = [(C_0 - C_e)/C_0] \times 100\% \quad (2)$$

### 2.2.3. Characterization

The samples were characterized by The Fourier transform infrared (FT-IR) spectra using KBr pressed disk technique were conducted by Perkin Elmer Spectrum 2000 Infrared spectrometer. M13 or MS and KBr were weighted and then were ground in an agate mortar for 10 min prior to pellet making. The spectrums were collected for each measurement over the spectral range of 400 - 4000  $cm^{-1}$ .

X-ray diffraction (XRD) analysis by Panalytical X'Pert Pro theta/theta with Kbeta radiation is filtered by a nickel, the operation voltage and current were kept at 40 kV and 40 mA, respectively.

TG thermograms were plotted using the multimodule 92-10 Setaram analyser operating from room temperature up to 1000°C in a  $Al_2O_3$  crucible, at 10°C/mn heating rate.

Nanomorphology was characterized by scanning electron microscopy (SEM). The SEM study was carried out using Hitachi S-4800 equipped with energy dispersive spectro- metry for chemical analysis (EDS) and operating at 15 kV acceleration voltages.

Concentrations of heavy metal ions were measured using an AA-100 Atomic Absorption Spectrometer (Varian).

## 3. Results and discussion

### 3.1. Modified Maghnite

The new bands at 3479 and 3410  $cm^{-1}$  for MS are representative of the symmetric and asymmetric stretching vibrations of the amino groups, suggesting that the silane coupling agent reacted with the -OH groups of M13.

The absorption band at  $2930\text{ cm}^{-1}$  corresponds to the C-H stretching vibration of  $\text{CH}_2$  groups of APTES. These observations clearly indicate the surface modification of M13 by APTES.

The XRD pattern of the MS was not changed by the surface modification (see fig.2).

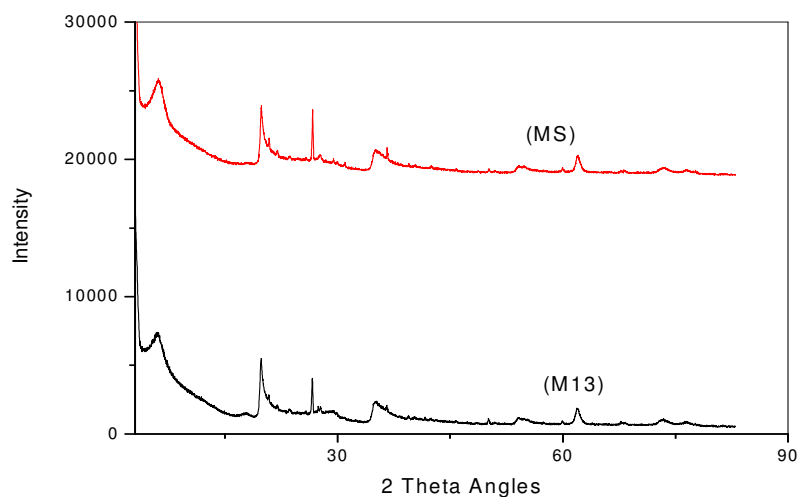


**Figure 2.** X-ray diffraction patterns of curves Maghnite (M13) and APTES–Maghnite (MS)

The SEM micrographs of M13 and MS were illustrated in Fig. 3. Obviously, the layer structure remained fine after the organic modification, and it could be observed that many small nanoparticles disappeared, probably due to the gathering force after modification. The surface appearance was slick for MS (b), much texture existed on the external surface layer pieces, and the small nanoparticles could be caused by the grafting and bonding process of APTES, which brought about a loose structure. MS showed a wide range of particle size, which was probably resulted from part of the destroyed structure and the different grafting degree during modification.

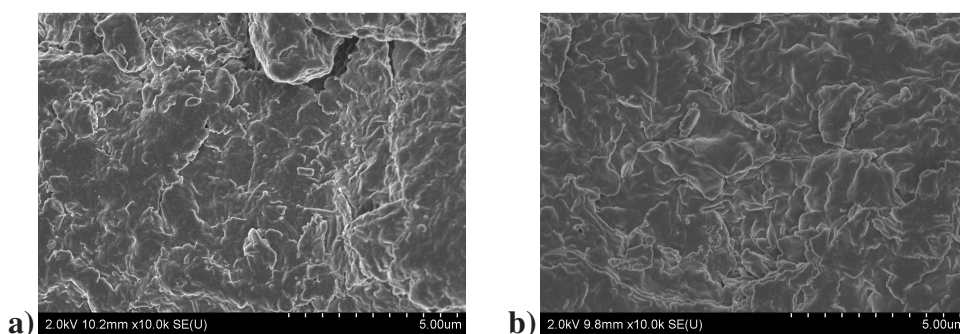


**Figure 3 .** The SEM of M13 (a) and MS (b).

### 3.2. Adsorption Studies

#### 3.2.1. Effect of Contact Time

Contact time was an important factor affecting adsorption. The adsorption experiments were carried out at different time intervals. As shown in Fig. 4, the adsorption processes for M13 and MS were so fast that the adsorption equilibrium was almost reached at the beginning. The adsorption on M13 and MS got equilibrium within 120 min and 300 min respectively, and then progressed slowly.

Two reasons could explain for the slow adsorption of  $\text{Zn(II)}$  on MMag. Firstly, it was difficult and slow for the MS to adsorb the  $\text{Zn(II)}$  in solution at beginning experiment; secondly, it was related to the hydrolysis of APTES with  $-\text{OH}$  grafting to M13. The grafting was hypothetically simulated as Fig.1. The triethoxysilane ( $-\text{Si}(\text{OC}_2\text{H}_5)_3$ ) of APTES hydrolyzed first during the adsorption, and then  $-\text{OH}$  connected to Mag.  $-\text{NH}_2$  hydrolysis before coordinating with  $\text{Zn(II)}$ , thus slowing down the removal rate. The possible processes were shown as Eqs. (3) and (4) [17]:

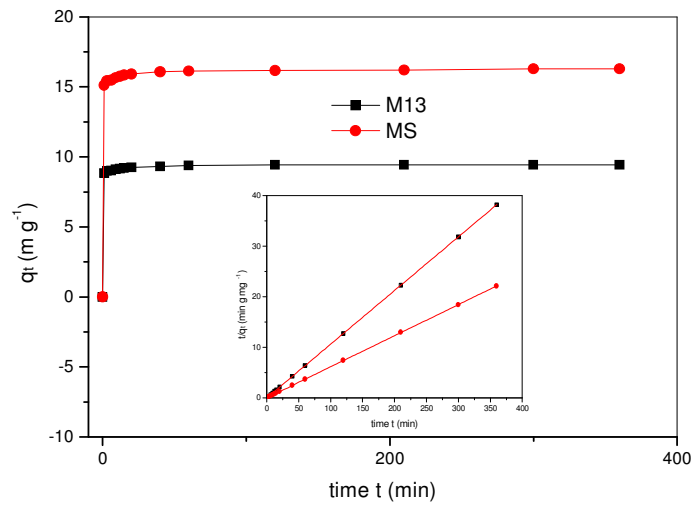
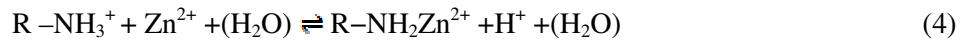


**Figure 4.** Effect of contact time and kinetic study of Zn(II) adsorption by Maghnite (M13) and modified maghnite (MS) (experimental conditions: 100mg/L Zn(II)for M13, 200mg/L Zn(II) for MS ; pH 9 for MS, pH 6.1 for M13).

### 3.2.2. Effect of Initial Concentration

The adsorption capacity plot of Zn(II) at different concentrations on M13 and MS was shown in Fig.5. The concentration range was set at 100-900 mg/L. The adsorption capacity increased with the increasing concentration. The adsorption equilibrium for M13 was first achieved at 400 mg/L. The removal process experienced two steps for MS. The adsorption capacity at 400 mg/L was twice of that at 190 mg/L, and then a slow increase followed until equilibrium at 600 mg/L. Thus, the experimental adsorption capacity of the adsorbent was chosen as 400 mg/L for M13 and 600mg/L for MS.

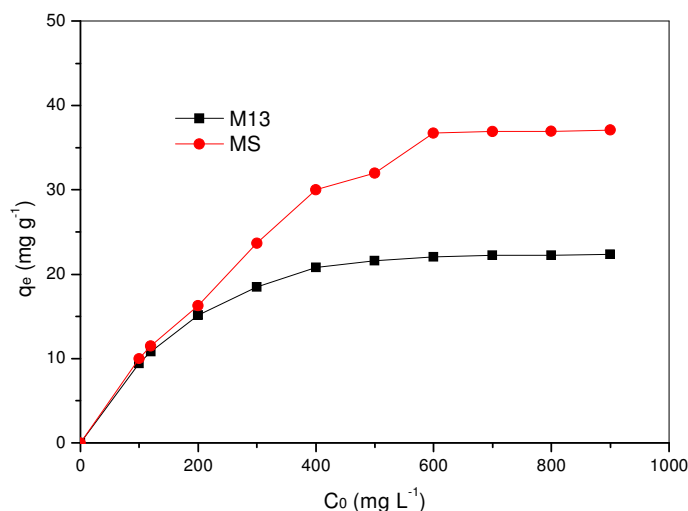


**Figure 5.** Effect of initial concentration and isotherm study of Zn(II) adsorption by maghnite (M13) and modified maghnite (MS).

### 3.2.3. Effect of Solution pH

Solution pH usually affected an adsorption process significantly. So a pH range of 1.0-10.0 was explored at certain Zn(II) concentrations and a contact time of 120 min, 300 min for M13, MS respectively.

The Zn(II) adsorption on MS was highly pH dependant. Fig.6 described the increased uptake with rising pH. In the strong acid solution, the adsorption was weak and even less than that of M13. Reasons for the phenomenon were discussed as follows: At low pH, H<sup>+</sup> was prior adsorbed on MS and thus causing competition with Zn(II). Excess H<sup>+</sup> took over the reactive adsorption sites on surface and also restrained the bonding of Zn(II). This was shown in Eq. (4) directly, which indicated that H<sup>+</sup> could push forward the reaction inversely. For MS, at high pH, OH<sup>-</sup> would promote the adsorption of Zn(II) by neutralizing the produced H<sup>+</sup> in reaction. MS was alkaline in water solution, so there is no need adding extra alkali to keep a high adsorption capacity.

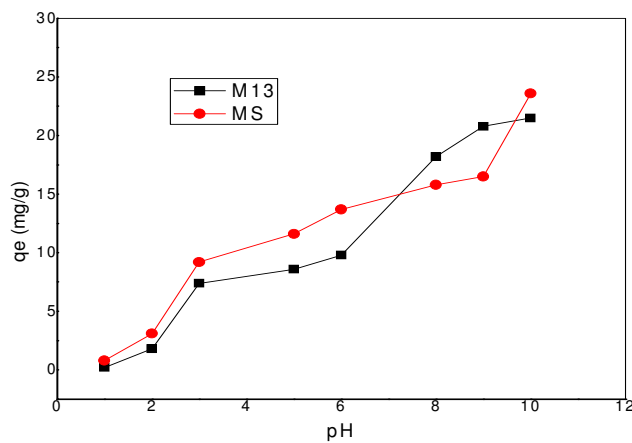


Figure 6. Effect of the pH on the  $q_e$ .

### 3.2.4. Kinetic Studies

Many models were used to describe the adsorption processes. The most appreciated were Pseudo-first-order (Eq. (5)), Pseudo-second-order (Eq. (6)) and Elovich model (Eq. (7)) [18]. As shown in Fig.4, the data corresponded to Pseudo-second-order well. The parameters of Pseudo-second-order were listed in Table 2. The coefficients of determination ( $R^2$ ) for two materials were good ( $>0.97$ ).

$$\ln(q_e - q_t) = \ln q_e - k_1 t \quad (5)$$

$$t/q_t = (1/k_2 q_e^2) + (1/q_e)t \quad (6)$$

$$q_t = (1/\beta) \ln(\alpha\beta) + (1/\beta)\ln t \quad (7)$$

where  $q_e$  (mg/g) and  $q_t$  (mg/g) are the adsorbed amounts of Zn(II) at equilibrium and time  $t$  (min);  $k_1$ ,  $k_2$  is the adsorption rate constants of Pseudo-second-order equation;  $\alpha$  (mg/(g.min)) is the initial adsorption rate and  $\beta$  (g/mg) is the chemical adsorption parameter.

Table 2. The Pseudo-first-order and the Pseudo-second-order parameters for Zn(II) onto maghnite (M13) and modified maghnite (MS).

Sample	Pseudo-first-order			Pseudo-second-order		
	$k_1$ [ $\text{min}^{-1}$ ]	$q_e$ [ $\text{mg g}^{-1}$ ]	$R^2$	$k_2$ [ $\text{g mg}^{-1} \text{min}^{-1}$ ]	$q_e$ [ $\text{mg g}^{-1}$ ]	$R^2$
M13	0.08	8.31	0.629	0.42	9.43	1
MS	0.27	14.98	0.752	0.16	16.28	0.999

### 3.2.5. Isotherm Studies

The equilibrium isotherm for Zn(II) adsorption at different concentrations was analyzed by Langmuir (Eq. (8)) (Langmuir, 1918) and Freundlich (Eq. (9)) (Freundlich, 1906), which were empirically used for heavy metals removal on soil and mixed components [19].

$$q_e = q_m (K_L C_e) / (1 + K_L C_e) \quad (8)$$

$$q_e = K_F C_e^n \quad (9)$$

where  $q_e$  (mg/g) is the adsorbed amount of Zn(II),  $C_e$  (mg/L) is the concentration of Zn(II) at equilibrium.  $K_L$ ,  $K_F$ ,  $n$  is the adsorption parameter decided by linear equation.  $q_m$  (mg/g) is the limited monolayer adsorption capacity. The linear equations of Langmuir and Freundlich were given as follows, respectively.

$$C_e/q_e = (1/q_m K_L) + (C_e/q_m) \quad (10)$$

$$\ln q_e = \ln K_F - n \ln C_e \quad (11)$$

The results of adsorption isotherm were shown in Fig.7. The adsorption capacity of Zn(II) on M13 was small in the whole period, which could be explained by the adsorption behavior described as surface complexation model at the low concentration, the surface adsorption was dominant at first [20].

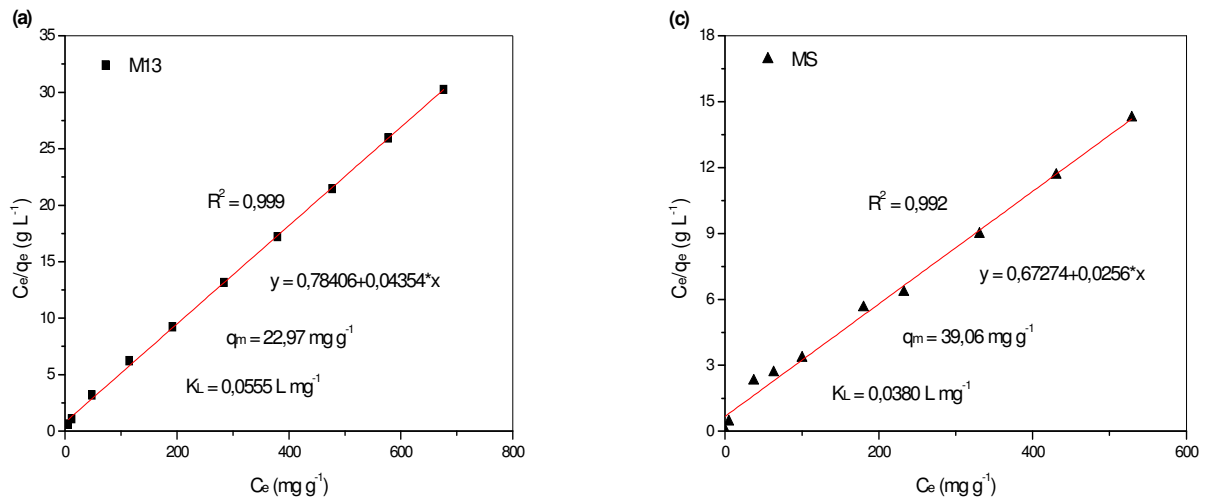


**Figure 7.** The Langmuir Linear plot for Zn(II) adsorption on M13 (a) and MS (b)

The  $q_e$  of the metal ions was increased with increasing concentrations until reaching equilibrium. The adsorption isotherm data for the metal ions were consistently better with Langmuir than Freundlich isotherms, which were determined by the correlation coefficients ( $R^2$ ). The maximum capacity ( $q_m$ ) for the metal ion calculated by the Langmuir equation differed for the two materials (Fig.7).

### 3.2.6. Comparison of maghnite clay (M13) and modified maghnite (MS) with various adsorbents for Zn(II) removal

The adsorption capacity of the M13 and MS clay for the removal of Zn(II) were compared with those of other adsorbents reported in literature and the values of adsorption capacities were presented in Table 3. The values reported in the form of monolayer adsorption capacity. The experimental data of the present investigation was comparable with the reported values. The maghnite clay and modified maghnite has a high adsorption capacity as comparable with that of the other adsorbents. Therefore, considering the low cost of this natural adsorbent, it can be used as an alternative material to minimize the concentration of Zn (II) in wastewater.

**Table 3.** Comparison of adsorption capacities of various adsorbents for Zn(II) metal ion.

Type of adsorbent	Adsorption capacities for Zn(II) [mg.g <sup>-1</sup> ]	Reference
-3-aminopropyltriethoxysilane -Maghnite (MS).	39.06	This work
- Natural Maghnites (M13).	22.97	This work
- Activated Alumina.	13.69	[21]
- Zeolite	13.20	[22]
- Natural Kaolin.	12.23	[20]
-Amphibolite.	11.50	[23]
- Active Carbon.	11.24	[24]
- Granite	08.64	[23]

## Conclusion

We describe the preparation and characterization of maghnite (M13) modified with 3-aminopropyltriethoxysilane (APTES) is excellent for removal of heavy metals ion such as  $Zn^{2+}$  from aqueous solution. The adsorption experiments showed that the removal of Zn(II) on MS was highly adsorbed ( $39.06 \text{ mg g}^{-1}$ ), while that on M13 was lower adsorbed ( $22.97 \text{ mg g}^{-1}$ ). Adsorption kinetics of two materials was in good agreement with Pseudo-second-order ( $R^2 > 0.99$ ). The Langmuir adsorption isotherm provided the best correlation with the adsorption data of M13 and MS. The results preliminarily implied that MS could be an effective adsorbent applied for Zn(II)-abundant wastewater. Further research is needed to determine the specific applications of the two adsorbents with respect to other pollutants and industrial wastewaters.

**Acknowledgements** - The authors gratefully acknowledge to the Dr Yves PILLET (Faculty of Sciences et Technology, group PGCM, University of Lorraine, Nancy, France) because of contribution to our study, and thankful for Joint Service Electronic Microscopy and Microanalysis at the University Henri Poincare of Nancy for MEB analysis. I appreciate Dr. Ghouti MEDJAHDI (Plasma nanoscience materials metal surfaces, institute Jean Lamour (IJL), Nancy university, France) to help and provide explanations by him on the DRX materials.

## References

1. Demirbas, A., *J. Hazard. Mater.* 157 (2-3) (2008) 220-229.
2. Lalhruaituanga, H., Jayaram, K., Prasad, M.N.V., Kumar, K.K., *Hazard, J. Mater.* 175 (1-3) (2010) 11-318.
3. Mohamad Ibrahim, M.N., Wan Ngah, W.S., Norliyana, M.S., Wan Daud, W.R., Rafatullah, M., Sulaiman, O., Hashim, R., *Hazard, J. Mater.* 182 (1-3) (2010) 77-385.
4. Zamzow, M.J., Eichbaum, B.R., Sandgren, K.R., Shanks, Sep, D.E., *Sci. Technol.* 25 (13-15) (1990) 1555-1569.
5. Castaldi, P., Santona, L., Enzo, S., Melis, P., *J. Hazard. Mater.* 156 (1-3) (2008) 428-434.
6. Kaya, A., Ören, A. H., *J. Hazard. Mater.* 125 (1-3) (2005) 183-189.
7. Karapinar, N., Donat, R., *Desalination.* 249 (1) (2009) 123-129.
8. Ijagbemi, C.O., Baek, M.H., Kim, D.S., *J. Hazard. Mater.* 166 (1) (2009) 538-546.
9. Meroufel B., Benali O., Benyahia M., Benmoussa Y., Zenasni M.A., *J. Mater. Environ. Sci.*, 4(3) (2013) 482-491
10. Tunali, S., Akar, T., Özcan, A.S., Kiran, I., Özcan, Sep, A., *Purif. Technol.* 47 (3) (2006) 105-112.
11. Uzun, H., Bayhan, Y.K., Kaya, Y., Cakici, A., Algur, O.F., *Desalination.* 154 (3) (2003) 233-238.
12. Huang, C.P., Huang, C.P., Morehart, A.L., *Water Res.* 24 (4) (1990) 433-439.
13. Ghorbel-Abid, I., Galai, M., Trabelsi-Ayadi, M., *Desalination.* 256 (2010) 190-195.
14. Ghorbel-Abid, I., Jrad, A., Nahdi, K., Trabelsi-Ayadi, M., *Desalination.* 246 (2009) 595-604.
15. Zenasni M. A., Benfarhi S., Mansri A., Benmehdi H., Meroufel B., Desbrieres J., Dedriveres R., *African Journal of Pure and Applied Chemistry*, 5(15) (2011) 486-493.
16. Muresanu M., Cioatera N., Trandafir I., Georgescu I., Fajula F., Galarneau A., *Microporous and Mesoporous Materials*, 146 (2011) 141-150.
17. Bradl H. B., *J. Colloid Interface Sci*, 277 (2004) 1-18.
18. Zhu M. X., Ding K. Y., Xu S. H., Jiang X., *J. Hazard. Mater.*, 165 (2009) 645-651.
19. Zenasni A. M., Benfarhi S., Merlin A., Molina S., George B., Meroufel B., *Natural Science*, 4 (2012) 856-868.
20. Meroufel B., Benali O., Benyahia M., Zenasni M. A., Merlin A., George B., *Journal of Water Resource and Protection*, 5 (2013) 669-680.
21. Bhattacharya A. K., Mandal S. N., Das S. K., *Chemical Engineering Journal*, 123(1-2) (2006) 43-51.
22. Katsou E., Malamis S., Tzanoudaki M., Haralambous K., Loizidou M., *Journal of Hazardous Material.* 189(3) (2011) 773-786.
23. Pérez-Novo C., Fernández-Calviño D., Bermúdez-Couso A., *Chemosphere*, 83(7) (2011) 1028-1034.
24. Mishra P. C., Patel R. K., *Journal of Hazardous Materials*, 168(1) (2009) 319-325.

(2015) ; <http://www.jmaterenvirosnci.com/>